Theoretical Investigation of Spin-Trapping Reactions

John Bentley* and Keith P. Madden

Contribution from the Radiation Laboratory, University of Notre Dame, Notre Dame, Indiana 46556-0579

Received December 2, 1993. Revised Manuscript Received August 22, 1994[⊗]

Abstract: The energetics of spin-trapping and related reactions, using nitrosomethane as a model spin trap, are examined using quantum chemical calculations at the MP2/6-31+G* level. It is established that nitrosomethane is a satisfactory model for the commonly employed spin trap 2-methyl-2-nitrosopropane. Free energy differences are reported for the reactions considered, using theoretically determined molecular structures and vibrational frequencies to convert molecular energies to room-temperature free energies. The effects of solvation are estimated by means of a self-consistent reaction field approach. The level of theory applied here is not expected to be quantitatively predictive, but it is expected to be of value in establishing energetic trends among possible reactions. Results reported here indicate that nitrosomethane dimer and the anion of the monomer are capable of reacting as spin traps, although less effectively than the monomer. In all cases, the ultimate product appears to be the nitroxide.

Introduction

The spin-trapping reactions of 2-methyl-2-nitrosopropane (MNP) have recently been systematically studied by time-resolved electron spin resonance (TRESR).[1] The MNP molecule is well-known to undergo dimerization under many conditions,[2] including the aqueous solutions of ref 1. The ESR spectra are consistent with undimerized MNP as the spin-trapping entity. However, pulse radiolytic studies by Kuwabara *et al.*[3] indicate that the MNP dimer is more efficient than the monomer in reacting with hydrated electrons. Furthermore, Madden and Taniguchi[4] have implicated the involvement of the MNP anion in the trapping of strongly reducing hydroxyalkyl radicals. The MNP anion has apparently been detected electrochemically.[5] The role, if any, of reduced or dimeric species in the spin-trapping process is an unresolved area currently being examined in this laboratory. It should be possible, using the methods of quantum chemistry, to identify the important transient species from a group of candidates and to characterize their roles in the chemistry of spin trapping for this widely used spin trap.

Because of the presence of the large (from a theoretician's perspective) *tert*-butyl moiety in the MNP molecule and its lack of participation in the reactions to be considered, it is desirable to substitute a smaller alkyl group for the *tert*-butyl group. We have selected nitrosomethane (NM) as a suitable substitute for MNP. In practice, NM and other primary and secondary nitrosoalkanes are not used as spin-trap molecules due to the tendency of their α-hydrogen to migrate to the oxygen, producing the corresponding oxime species,[6] as well as to the higher stability in aqueous solution of dimers of the primary and secondary nitrosoalkanes relative to tertiary systems.[7] These drawbacks do not hinder the use of NM as a theoretical model, of course.

Previous theoretical work has been carried out involving nitrosomethane,[8−11] its dimer,[12−14] and various nitroxides.[15−18] However, the thrust of the nitrosomethane studies has been to interpret its electronic spectrum, while the nitroxides have been studied in order to compare with experimental hyperfine coupling constants. Prior to a very recent report by Boyd and Boyd,[19] no theoretical attention had focused on the spin-trapping process itself, or on the possible transients in radiolyzed solutions. The Boyds' study differs from ours in looking at a different set of nitroso adducts and asking about the stability of the adducts as a function of radical electronegativity. Although some of the molecules of interest to us have previously been examined in greater computational detail than we employ here, they have been studied as isolated systems and the results do not directly bear on the questions we are asking.

The paper is organized as follows. In the second section, we describe the theoretical procedures to be applied. In the third section, we compare computed molecular structures and vibrational frequencies to available experimental data. In the fourth section, we establish that nitrosomethane is indeed a satisfactory model system for 2-methyl-2-nitrosopropane, both in its molecular properties and in its energies of reaction. In the fifth section, we apply the described methods to a number of reactions involving NM, its anion, its dimer, and other derivatives. Finally, we summarize our conclusions concerning the possible reactions involved in and competing with spin trapping.

[⊗] Abstract published in *Advance ACS Abstracts*, November 1, 1994.

(1) Madden, K. P.; Taniguchi, H. *J. Am. Chem. Soc.* **1991**, *113*, 5541−5547.
(2) Gowenlock, B. G.; Lüttke, W. *Quart. Rev.* **1957**, *12*, 321−340.
(3) Kuwabara, M.; Hiraoka, W.; Sawamura, S.; Katayama, M. *J. Am. Chem. Soc.* **1991**, *113*, 3995−3997.
(4) Madden, K. P.; Taniguchi, H. *Appl. Radiat. Isot.* **1993**, *44*, 449−453.
(5) McIntire, G. L.; Blount, H. N.; Stronks, H. J.; Shetty, R. V.; Janzen, E. G. *J. Phys. Chem.* **1980**, *84*, 916−921.
(6) Smith, P. A. S. *The Chemistry of Open-Chain Organic Nitrogen Compounds*; W. A. Benjamin, Inc.: New York, 1966; Vol. II.
(7) Batt, L.; Gowenlock, B. G. *J. Chem. Soc., Faraday Trans.* **1960**, *1960*, 1022−1027.
(8) Ha, T.-K.; Wild, U. P. *Chem. Phys.* **1974**, *4*, 300−306.
(9) Ernsting, N. P.; Pfab, J.; Römelt, J. *J. Chem. Soc., Faraday Trans. 2* **1978**, *74*, 2286−2294.
(10) Adeney, P. D.; Bouma, W. J.; Radom, L.; Rodwell, W. R. *J. Am. Chem. Soc.* **1980**, *102*, 4069−4074.
(11) Cimiraglia, R.; Persico, M.; Tomasi, J. *J. Am. Chem. Soc.* **1985**, *107*, 1617−1622.
(12) Heiberg, A. B. *Chem. Phys.* **1979**, *43*, 415−423.
(13) Minato, T.; Yamabe, S.; Oda, H. *Can. J. Chem.* **1982**, *60*, 2740−2748.
(14) Lüttke, W.; Skancke, P. N.; Traetteberg, M. *Theor. Chim. Acta* **1994**, *87*, 321−333.
(15) Davis, T. D.; Christoffersen, R. E.; Maggiora, G. M. *J. Am. Chem. Soc.* **1975**, *97*, 1347−1354.
(16) Gillon, B.; Becker, P.; Ellinger, Y. *Mol. Phys.* **1983**, *48*, 763−774.
(17) Gillon, B.; Ellinger, Y. *Mol. Phys.* **1988**, *63*, 967−979.
(18) Takase, H.; Kikuchi, O. *Chem. Phys.* **1994**, *181*, 57−62.
(19) Boyd, S. L.; Boyd, R. J. *J. Phys. Chem.* **1994**, *98*, 1856−1863.

0002-7863/94/1516-11397$04.50/0

Computational Procedures

All calculations reported here have been carried out with the GAUSSIAN 88,[20] GAUSSIAN 90,[21] and GAUSSIAN 92[22] suites of quantum chemistry programs running on Convex C-120 and C-240 computers. Three levels of theory are employed. In the first, the Hartree–Fock–Roothaan equations are solved using a standard basis set[23] designated 6-31+G and described as split valence with diffuse functions. This basis set was designed for use with anions; we use it for all species studied here for consistency. Restricted (RHF) or unrestricted (UHF) self-consistent field wave functions are employed depending on whether the molecule has a singlet or doublet electronic state. For each molecule examined, the equilibrium molecular structure is determined using the gradient-searching algorithms incorporated in the GAUSSIAN programs. All energies reported below are based on electronic energies calculated at the equilibrium structures. This level of theory will be referred to below as SCF.

Molecular vibrational frequencies are computed at the SCF level for most of the molecules considered here. Unpublished tests by the authors on a number of small molecules indicate that the 6-31+G basis set predicts frequencies very similar to those predicted by the closely related (and well characterized) 6-31G* basis set.[24] It has been recommended[25] that frequencies predicted by the latter basis set be scaled by 0.8929 before comparison with experimental frequencies, in order to compensate for known deficiencies in the theoretical model. The same factor will be applied to all theoretical frequencies reported in this paper.

The second level of theory to be used employs the 6-31+G* basis set, which provides polarization functions (d-type basis functions) on C, N, and O. It also incorporates some electron correlation into the molecular wave function by applying Møller–Plesset perturbation theory through second order.[26] The molecular structure is reoptimized in the presence of the correlation terms. This level is refered to as MP2. As above, the wave functions are restricted (RMP2) or unrestricted (UMP2) depending on the spin state of the molecule.

The third level to be used is the Gaussian-2 (G2) theory of Pople and co-workers.[27] G2 attempts to provide quantitatively accurate energies (i.e., to within 10 kJ mol^{-1} of experiment) by starting with a useful but economical basis set and correlation procedure and adding corrective terms to deal with deficiencies in the basis set and higher-order contributions to the correlation energy. In work published to date G2 has been generally successful in meeting its goal. Its drawback for our purposes is that it is computationally quite demanding. In the present work, we apply it only to nitrosomethane and closely related molecules, using it to assess the accuracy of the more approximate SCF and MP2 results.

The SCF energy calculations are not reported in this paper. The lack of d-type (polarization) basis functions makes the 6-31+G basis set too inflexible to provide a consistent representation of the energies of the molecules dealt with here. Consequently, considerable shifts in free energies of reaction are noted between the SCF results and the MP2 results. In general, however, the MP2 free energies tend to be within 50 kJ mol^{-1} of the G2 values. We emphasize that calculations at the MP2/6-31+G* level are not expected to provide quantitative predictions (i.e., with an accuracy of 10 kJ mol^{-1} or better). Instead, we will focus on the trends in free energies and reactivities, which we expect to persist in more extensive calculations.

At all levels, thermodynamic quantities such as free energies of reaction are calculated from theoretically derived data.[28] These quantities are based on the electronic energies, the (scaled) SCF vibrational frequencies, the computed equilibrium molecular structures, and the rigid rotor and harmonic oscillator approximations.

Free energies of hydration (ΔG_{hydr}) are computed using a self-consistent reaction field (SCRF) algorithm[29] programmed in GAUSSIAN 92. In the most general form of SCRF, the molecule to be solvated is enclosed in a sphere or ellipsoid, outside of which is a continuum dielectric material with the static dielectric constant of the solvent. The various multipole moments of the solute molecule induce an electric field in the continuum, which in turn perturbs the charge density of the solute molecule. The wave function of the solute molecule is recomputed in the presence of the reaction field, leading to new multipole moments and a new reaction field. This process repeats to self-consistency. Some implementations take this procedure to high orders of the solute molecular multipole moments, e.g., Medina-Llanos *et al.*[30] use $l \leq 10$, while Rivail and Rinaldi[31] use $l \leq 6$. The implementation provided in GAUSSIAN 92[29] truncates the multipole expansion at the dipole level (i.e., $l = 0, 1$). In this implementation,[29] the energy of the system is expressed as

$$E(\mathrm{SCRF}) = \langle\psi|H^0|\psi\rangle - {}^1/_2(1 - \epsilon^{-1})Q^2/a_0 - {}^1/_2 g\langle\psi|\mu|\psi\rangle\langle\psi|\mu|\psi\rangle \quad (1)$$

in which H^0 is the Hamiltonian for the gas-phase solute molecule, $g = 2a_0^{-3}(\epsilon - 1)/(2\epsilon + 1)$, a_0 is the radius of the spherical cavity, ϵ is the solvent dielectric constant (taken to be 78.4 in this work), ψ is the solute wave function in the presence of the solvent reaction field, Q is the net charge, if any, on the solute molecule, and μ is the dipole moment operator. Because the dipole moment of an ion is not translationally invariant, the center of the cavity sphere is placed at the center of charge of the solute molecule to be consistent with the spherical cavity model.[29] The second term on the right-hand side of eq 1 is the Born term for the free energy of solvation of a spherical ion.

The SCRF method described above is not a complete picture of the solvation process. It incorporates only electrostatic interactions between solute and solvent and neglects dispersion, repulsion, and exchange interactions, as well as the energy expended in creating a cavity in the solvent medium. Dispersion and cavitation are introduced by means of a model to be introduced below. Repulsion and exchange are ignored at this level of theory. Hydrogen bonds between solute and solvent are not dealt with directly by SCRF methods. However, because hydrogen bonding has a very large electrostatic component, SCRF methods are able to account for a substantial part of its energetic contribution to solvation.[32] In any case, the reader should be aware of the potential deficiency.

Initially we employed the solute sphere radii recommended by Wong, Wiberg, and Frisch[33] (WWF) and computed by GAUSSIAN 92. All hydration energies were computed at the SCF level with the 6-31+G basis set at the gas-phase optimized geometries. As WWF point out, the energies computed in the SCRF approximation combine the internal energy contribution of the solute molecule with the free energy of

(20) Gaussian 88; Frisch, M. J.; Head-Gordon, M.; Schlegel, H. B.; Raghavachari, K.; Binkley, J. S.; Gonzales, C.; DeFrees, D. J.; Fox, D. J.; Whiteside, R. A.; Seeger, R.; Melius, C. F.; Baker, J.; Martin, R. L.; Kahn, L. R.; Stewart, J. J. P.; Fluder, E. M.; Topiol, S.; Pople, J. A.; Gaussian, Inc.: Pittsburgh, PA, 1988.

(21) Gaussian 90; Frisch, M. J.; Head-Gordon, M.; Trucks, G. W.; Foresman, J. B.; Schlegel, H. B.; Raghavachari, K.; Robb, M.; Binkley, J. S.; Gonzales, C.; DeFrees, D. J.; Fox, D. J.; Whiteside, R. A.; Seeger, R.; Melius, C. F.; Baker, J.; Martin, R. L.; Kahn, L. R.; Stewart, J. J. P.; Topiol, S.; Pople, J. A.; Gaussian, Inc.: Pittsburgh, PA, 1990.

(22) Gaussian 92; Frisch, M. J.; Trucks, G. W.; Head-Gordon, M.; Gill, P. M. W.; Wong, M. W.; Foresman, J. B.; Johnson, B. G.; Schlegel, H. B.; Robb, M. A.; Replogle, E. S.; Gomperts, R.; Andres, J. L.; Raghavachari, K.; Binkley, J. S.; Gonzales, C.; Martin, R. L.; Fox, D. J.; DeFrees, D. J.; Baker, J.; Stewart, J. J. P.; Pople, J. A.; Gaussian, Inc.: Pittsburgh, PA, 1992.

(23) Frisch, M. J.; Pople, J. A.; Binkley, J. S. *J. Chem. Phys.* **1984**, *80*, 3265.

(24) Hariharan, P. C.; Pople, J. A. *Theor. Chim. Acta* **1973**, *28*, 213.

(25) Pople, J. A.; Schlegel, H. B.; Krishnan, R.; DeFrees, D. J.; Binkley, J. S.; Frisch, M. J.; Whiteside, R. A.; Hout, R. J.; Hehre, W. J. *Int. J. Quantum Chem., Symp.* **1981**, *S15*, 269.

(26) Møller, C.; Plesset, M. S. *Phys. Rev.* **1934**, *46*, 618.

(27) Curtiss, L. A.; Raghavachari, K.; Trucks, G. W.; Pople, J. A. *J. Chem. Phys.* **1991**, *94*, 7221–7230.

(28) Lewis, G. N.; Randall, M. *Thermodynamics*, 2nd ed.; revised by K. S. Pitzer and L. Brewer; McGraw-Hill, Inc.: New York, 1961; pp 419–449.

(29) Wong, M. W.; Wiberg, K. B.; Frisch, M. J. *J. Chem. Phys.* **1991**, *95*, 8991–8998.

(30) Medina-Llanos, C.; Ågren, H.; Mikkelsen, K. V.; Jensen, H. J. A. *J. Chem. Phys.* **1989**, *90*, 6422–6435.

(31) Rivail, J. L.; Rinaldi, D. *Chem. Phys.* **1976**, *18*, 233.

(32) Ford, G. P.; Wang, B. *J. Am. Chem. Soc.* **1992**, *114*, 10563–10569.

(33) Wong, M. W.; Wiberg, K. B.; Frisch, M. J. *J. Am. Chem. Soc.* **1992**, *114*, 1645–1652.

solute−solvent interaction and solvent rearrangement. To convert the SCRF energies to free energies, one must include the contributions of the internal degrees of freedom, much as is done for the gas-phase systems. WWF contend[29] that this can be done using ideal-gas translational and rotational terms and harmonic oscillator vibrational frequencies, all computed at a molecular geometry reoptimized in the presence of the SCRF. Our tests indicated that, for the molecules studied here, the geometry reoptimization changed the free energy of hydration by less than 2 kJ mol^{-1}, an insignificant quantity on the scale of reaction energies of interest here. Thus, to a satisfactory approximation, the contributions to the free energy from internal degrees of freedom cancel between the gas and solution phases, and we arrive at

$$\Delta G^\circ_{hydr}(\text{SCRF; 298K}) = E(\text{SCRF}) - E(\text{gas phase}) + G_{cavitation} + G_{dispersion} + RT\ln(\varrho_{soln}/\varrho_{gas}) \quad (2)$$

as a theoretical description of the free energy of hydration at this level of approximation. The last term of eq 2 is the concentration factor due to converting from the gas-phase standard state of 1 atm to the solution standard state of 1 M solution, in which ϱ is the density of solute in the indicated phase. This term has a value of 8 kJ mol^{-1} at 298 K. The free energies of solute cavity formation and solute−solvent dispersion interaction are approximated from the work of Hermann[34] and Floris and Tomasi,[35] respectively, adapting relationships they presented between the free energy components and the cavity surface areas. The resulting expression is

$$G_{cavitation} + G_{dispersion} = 0.787a_0^2 + 2.9 \quad (3)$$

in which G is given in kJ mol^{-1} and a_0 in Å. This expression was derived from data on aliphatic hydrocarbons, so some error will accrue when it is applied to the varied assortment of molecules considered here. However, since $G_{cavitation} + G_{dispersion}$ is on the order of 5−10 kJ mol^{-1} for these molecules, the contribution to the total error from this source will be slight. Note that eq 3 is only valid in the domain in which it was fit, and becomes less accurate for molecules the size of methane or smaller.

Free energies of hydration for neutral organic molecules tend to cluster in the range between +15 and −30 kJ mol^{-1}.[36] Hydration free energies for ions are generally large and negative, and show a reciprocal dependence on molecular size,[37,38] as the Born energy implies. In the course of applying SCRF to the molecules under study here, we discovered that values of ΔG°_{hydr} for charged molecules were generally about 40% lower than our expectations based on experimental hydration free energies of comparably sized molecules. We computed ΔG°_{hydr} for a number of ionic species in the compilation of Pearson[38] and observed that the consistent differences between experiment and our calculations arose from our use of the WWF sphere radii a_0. The WWF radii put the cavity surface significantly farther from the solute molecule (i.e., roughly 0.6 Å) than do the van der Waals atomic radii used by other workers to produce nonspherical cavities (for example, see Miertus *et al.*[39]). This leads to a weaker interaction between the molecule and the dielectric continuum, and thus a less negative free energy of hydration. We found that a radius derived from the volume enclosed by the 0.001 e/bohr^3 electron density contour provided a satisfactory approximation to experimental hydration energies for neutral molecules. (The relationship between this definition of a_0 and that of WWF is $a_0(\text{WWF}) = 1.1a_0(0.001) + 0.5$ Å.) For ions, we observed that a radius 0.2 Å less than $a_0(0.001)$ gave best overall agreement with experiment. This observation is consistent with recent experience in determining atomic radii for nonspherical solute cavities.[40] For a set of 25 molecules with experimentally known free energies of hydration,[38] this set of radii produces an average absolute error of 8 (neutrals) and 24 kJ mol^{-1} (ions). We recalculated all hydration free energies with this set of radii in place of the WWF values, and these are the results reported in Table 3.

Table 1. Structural Parameters (bond lengths in Å, angles in deg) of Nitrosomethane Monomer and 2-methyl-2-nitrosopropane Dimer

	experiment	SCF	MP2
Nitrosomethane			
NO bond length	1.211	1.202	1.235
CN bond length	1.480	1.468	1.475
CH bond length (in plane)	1.094	1.080	1.093
CH bond length (out of plane)	1.094	0.081	1.094
CNO bond angle	113.2	115.4	112.8
HCN bond angle (in plane)	111.0	111.4	111.4
HCN bond angle (out of plane)	107.2	107.3	106.8
MNP *Trans* Dimer			
NO bond length	1.265(2)	1.318	
NN bond length	1.309(2)	1.243	
CN bond length	1.533(2)	1.540	
C_1C_2 bond length (in plane)	1.522(3)	1.531	
C_1C_3 bond length (out of plane)[a]	1.511(4)	1.535	
C_1C_4 bond length (out of plane)[a]	1.509(4)		
NNO bond angle	120.4(2)	120.6	
NNC bond angle	119.9(1)	122.2	
NC_1C_2 bond angle (in plane)	108.5(2)	106.7	
NC_1C_3 bond angle (out of plane)[a]	106.1(2)	108.7	
NC_1C_4 bond angle (out of plane)[a]	109.0(2)		

[a] The indicated structural features are equivalent in the gas-phase calculations. In the crystal environment, however, the molecule no longer possesses a symmetry plane.

The gas-phase energies of the various molecules are combined with the free energies of hydration to produce free energies of reaction in solution, which are reported in Table 4. It is well documented[41,42] that reactions in which the total number of paired electrons is not held constant require more care in their theoretical treatment to achieve a high level of accuracy. Several reactions in Table 4 (e.g., reactions 8 through 11) are of this type. The description of these nonisogyric reactions would be of concern if we were attempting to reach chemical accuracy (errors of less than 10 kJ mol^{-1}). In the present circumstances, it is not an issue, since the expected errors[41] are not large enough to interfere with the trends of reactivity that we note.

At the level of theory described above, the expected average error in free energies of hydration is no greater than that of the gas-phase free energies reported here, and thus suitable for our goal of discovering trends in spin-trap reactivity. Quantitative prediction of free energies of reaction in solution will require both a more elaborate quantum mechanical description of the gas-phase molecules and SCRF implementations with more realistic cavities and more complete interaction terms.[32,39,43]

Comparison with Experiment

Experimentally determined molecular structures have been reported for the NM monomer (determined by microwave spectroscopy[44]) and the MNP dimer (determined by x-ray crystallography[45]). Experimental structure parameters are collected in Table 1 and compared with the SCF and MP2 theoretical parameters. The general structures of these and closely related molecules are shown in Figure 1.

For nitrosomethane the agreement between experiment and both levels of theory is generally satisfactory. For the MNP dimer, an obvious difficulty appears in the large differences of the theoretical NO and NN bond lengths from the experimental values: The calculated NO bond length is 0.06 Å longer than the experimental, whereas that for NN is almost 0.07 Å shorter.

(34) Hermann, R. B. *J. Comp. Chem.* **1993**, *14*, 741−750.
(35) Floris, F.; Tomasi, J. *J. Comp. Chem.* **1989**, *10*, 616−627.
(36) Hine, J.; Mookerjee, P. K. *J. Org. Chem.* **1975**, *40*, 292−298.
(37) Marcus, Y. *J. Chem. Soc., Faraday Trans.* **1991**, *87*, 2995−2999.
(38) Pearson, R. G. *J. Am. Chem. Soc.* **1986**, *108*, 6109−6114.
(39) Miertus, S.; Scrocco, E.; Tomasi, J. *Chem. Phys.* **1981**, *55*, 117.
(40) Orozco, M.; Luque, F. J. *Chem. Phys.* **1994**, *182*, 237−248.
(41) Pople, J. A.; Luke, B. T.; Frisch, M. J.; Binkley, J. S. *J. Phys. Chem.* **1985**, *89*, 2198−2203.
(42) Pople, J. A.; Schleyer, P. v. R.; Kaneti, J.; Spitznagel, G. W. *Chem. Phys. Lett.* **1988**, *145*, 359−364.
(43) Cramer, C. J.; Truhlar, D. G. *J. Am. Chem. Soc.* **1991**, *113*, 8305−8311.
(44) Turner, P. H.; Cox, A. P. *J. Chem. Soc., Faraday Trans. II* **1978**, *74*, 533−559.
(45) Gowenlock, B. G.; McCullough, K. J.; Manson, R. B. *J. Chem. Soc., Perkin Trans. II* **1988**, 701−703.

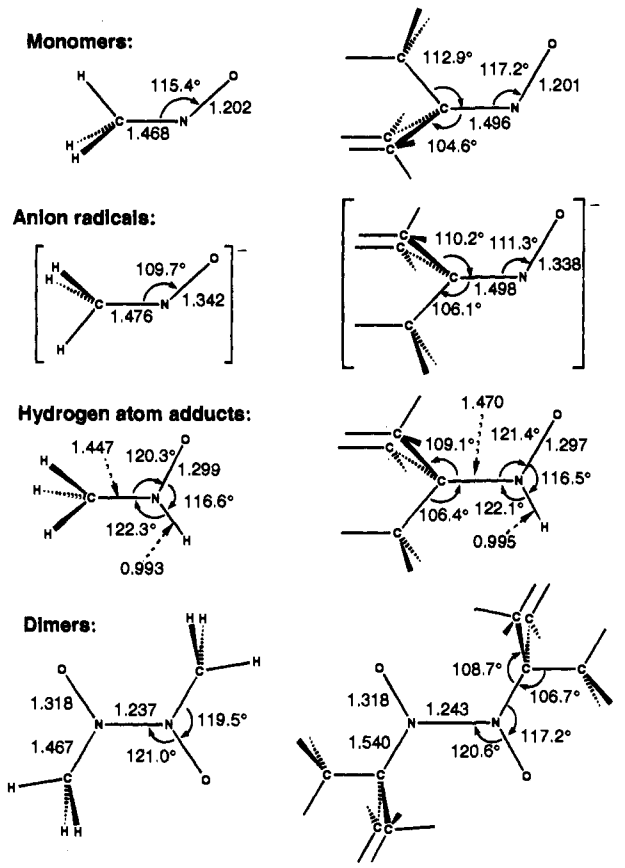

Figure 1. Optimized (SCF) molecular geometries of nitrosomethane and 2-methyl-2-nitrosopropane, along with their anions, hydrogen adducts, and *trans* dimers. In the monomers and anions, the CNO structure defines a symmetry plane. In the hydrogen adduct CH_3NHO, the adduct hydrogen is about 10° out of the CNO plane and the nearest methyl hydrogen has a dihedral angle of 48° from the oxygen. In $(CH_3)_3CNHO$, on the other hand, bonding is planar at nitrogen and the point group is C_s. The central framework of both dimers is planar, giving them C_{2h} symmetry. The rearmost hydrogen atom is hidden in each *tert*-butyl group.

The calculation essentially reverses the relative bond lengths (and strengths) of NN and NO. The *tert*-butyl parameters are in satisfactory agreement, as expected from their relative isolation from the ONNO framework of the molecule. Structural parameters involving hydrogen have not been compared, since the experimental values show considerable perturbation by the crystal environment. Although we have not carried out MP2 calculations on $(MNP)_2$, we can examine the corresponding bond lengths in the SCF and MP2 structures of the $(NM)_2$ dimer to see how closely the MP2 computations follow experiment. For $(NM)_2$ we have r_{NO}(SCF) = 1.318 Å and r_{NN}(SCF) = 1.237 Å, both very close to the SCF values for $(MNP)_2$. At the MP2 level, the $(NM)_2$ bond lengths are r_{NO} = 1.269 Å and r_{NN} = 1.354 Å. The 0.117 Å shift in the NN bond length indicates that the SCF and MP2 levels give qualitatively different pictures of the bonding in the ONNO fragment. While the MP2 r_{NO} bond length in $(NM)_2$ is satisfactorily close to the experimental value for $(MNP)_2$, the r_{NN} value is too large by almost 0.05 Å, indicating that the MP2 calculation still has deficiencies for this system. In a recent theoretical study of the dimerization of HNO, Lüttke, Skancke, and Traetteberg[14] showed that geometry determination at the QCISD level and energy calculation at the MP4(SDTQ) level suffice to resolve the problems described above.

Experimental infrared spectra have been reported for NM and *trans*-$(MNP)_2$, the former in argon matrix and the latter in Nujol.

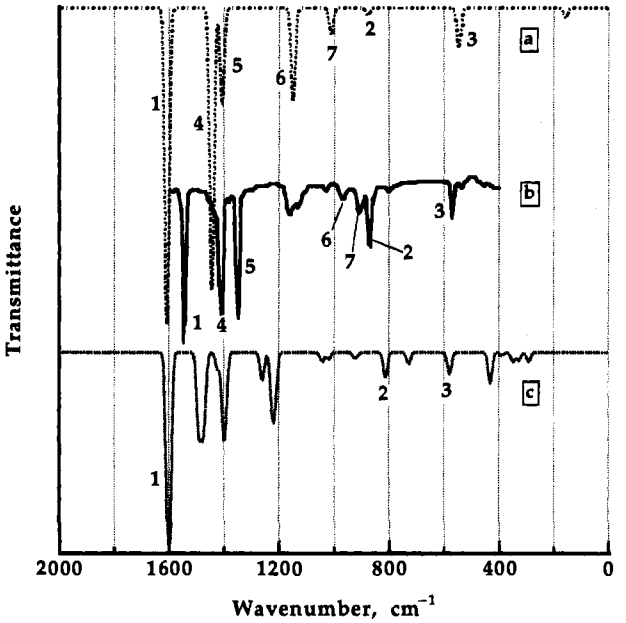

Figure 2. Infrared vibrational spectra of nitrosomethane and 2-methyl-2-nitrosopropane: (a) theoretical spectrum of NM; (b) experimental spectrum in argon matrix of NM, from Barnes *et al.*[46] (reproduced by permission of the Royal Society); (c) theoretical spectrum of MNP. Theoretical wavenumbers and intensities of IR absorption lines have been calculated from the HF/6-31+G wave functions, and all wavenumbers have been scaled by 0.8929. To assist in visual interpretation, the stick spectra have been convoluted with a Gaussian function that gives each line a 30 cm^{-1} full-width at half-maximum and provides proportionality between calculated line intensity and integrated area. The overall amplitudes of the spectra are arbitrary. Spectrum assignments are the following: (1) NO stretch; (2) CN stretch; (3) CNO bend; (4) CH_3 asymmetric deformation; (5) CH_3 symmetric deformation; (6) symmetric CH_3 rock; (7) asymmetric CH_3 rock. Unassigned lines in spectrum (b) arise from species other than nitrosomethane; unassigned lines in spectrum (c) arise from the *tert*-butyl group.

In Figure 2, the experimental spectrum of NM reported by Barnes, Hallam, Waring, and Armstrong[46] is compared with the present calculations. Peaks 1, 2, and 3 involving the CNO fragment and 4 and 5 involving the methyl groups are reproduced rather well by the theory. Peaks 6 and 7, the methyl rocking modes, are considerably shifted (100–200 cm^{-1}) by the theory relative to the experimental assignments. Additional peaks in the experimental spectrum, especially the broad band around 1150 cm^{-1}, arise from other products of the photolysis reaction used to produce nitrosomethane, according to Barnes *et al.* However, Dognon, Pouchan, and Dargelos[47] argue, based on SCF/4-31G calculations of vibrational force constants, that the line at 1150 cm^{-1} is the methyl in-plane rocking mode and that Barnes' line at 967 cm^{-1} is actually a dimer band. The present calculations are not sufficiently reliable to resolve this question.

Comparison of 2-Methyl-2-nitrosopropane and Nitrosomethane

In order to assess the effect of the *tert*-butyl group on the interactions of MNP we have calculated, at the SCF level, the gas-phase energies of MNP reduction, dimerization, and trapping of hydrogen atom and compared these quantities to the

(46) Barnes, A. J.; Hallam, H. E.; Waring, S.; Armstrong, J. R. *J. Chem. Soc., Faraday Trans.* **1976**, 1–10.
(47) Dognon, J. P.; Pouchan, C.; Dargelos, A. *Chem. Phys. Lett.* **1983**, *99*, 316–321.

Table 2. Energies of Reaction (in kJ mol^{-1}) for Simple Reactions Involving Nitrosomethane and 2-Methyl-2-nitrosopropane

reaction	energy of reaction[a] NM	MNP
reduction ($A + e^- \rightarrow A^-$)	−25	−29
spin trapping ($A + H \rightarrow AH$)	−306	−304
dimerization ($2A \rightarrow A_2$)	−35	15

[a] Energies of reaction are computed as product electronic energies minus sums of reactant electronic energies. All calculations in this table are at the SCF level.

corresponding quantities for NM. The structures of the corresponding systems are presented in Figure 1.

The geometries of NM and MNP shown in Figure 1 are essentially similar. NO bond lengths are almost identical. The greater steric repulsion between the *cis* methyl group and the oxygen leads to a 0.028 Å lengthening of the CN bond and 2° changes in the CNO and CCN bond angles. Much the same trends are observed in the radical anions NM^- and MNP^-, and the shifts that occur in the reduced form of MNP relative to the parent are closely mirrored in the shifts occurring in NM^-. The hydrogen atom adducts MNPH and NMH repeat this pattern, with two differences: In MNPH the methyl groups are *gauche* and *trans* to the oxygen, whereas in NMH the dihedral angle of the methyl hydrogen nearest to the oxygen is 45°; in MNPH the hydrogen bound to nitrogen is in the CNO plane, whereas in NMH it is 12° out of the plane. The $(CNO)_2$ frameworks in the two dimeric structures are quite similar to each other, except that the CN bond length is 0.07 Å longer in $(MNP)_2$ than in $(NM)_2$, a more pronounced difference than in the various monomeric species.

The gas-phase energies of reduction, hydrogen trapping, and dimerization of NM and MNP appear in Table 2. The trends observed in MNP are reproduced in the smaller system, except for the energy of dimerization. In this instance, it is not possible to confirm that the stationary point found for the MNP dimer by the program is indeed a minimum, since our computing resources are insufficient to determine the vibrational frequencies of a system this large. The calculated positive gas-phase dimerization energy of MNP is contrary to observation for this species. It will be seen in a later section that the calculation of dimer energies poses some problems at the levels of theory employed here.

Finally, we compare the vibrational spectra of the NM- and MNP-derived species with each other in Figures 2–4 for the parent species, their anions, and their hydrogen adducts, respectively. We could not obtain vibrational frequencies for MNP dimer and so cannot extend the comparison to that case. In each case we concentrate on the vibrational frequencies that are associated with the CNO framework of the molecule, and are labeled 1 for NO stretch, 2 for CN stretch, and 3 for CNO bend. For NM, ν_1 and ν_3 are relatively unaffected by the methyl/*tert*-butyl substitution, whereas the CN stretch mode moves to lower frequency, reflecting the longer CN bond length in MNP. In the anions (Figure 3), the NO stretch in NM^- is distributed between two bands, one 110 cm^{-1} lower and the other 50 cm^{-1} higher than in MNP^-. This is due to an accidental degeneracy with the methyl rocking band, which mixes the character of the two vibrations. In NMH and MNPH (Figure 4), the ν_1 lines are again essentially similar. The figures indicate that the characteristic bands having to do with the CNO skeleton are relatively independent of the nature of the hydrocarbon substituent and vary regularly with the particular modification of the CNO fragment. In particular, the NO stretching frequency is a sensitive indicator of the extent of reduction of the molecule, varying from 1607 cm^{-1} in NM to

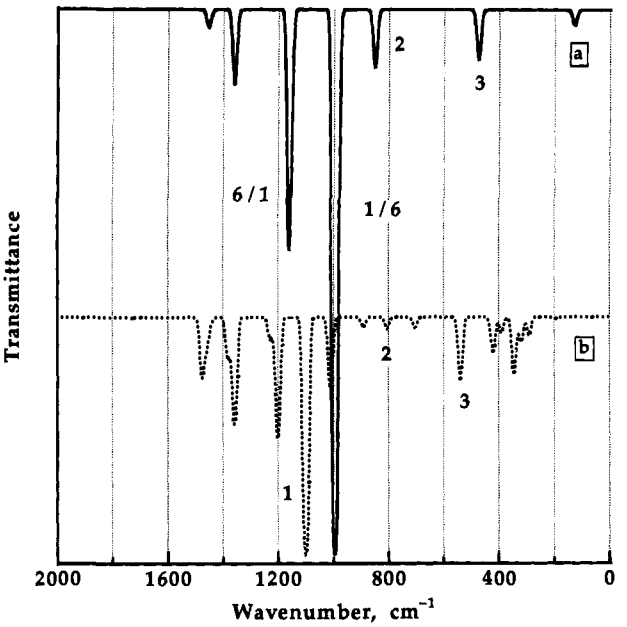

Figure 3. Calculated infrared vibrational spectra of (a) nitrosomethane anion and (b) 2-methyl-2-nitrosopropane anion. Spectra have been converted from stick spectra by the same procedure as in Figure 2. Assigned lines in the spectra are (1) NO stretch, (2) CN stretch, and (3) CNO bend. In part a, the NO stretch mode is accidentally degenerate with a CH_3 rocking mode, so both of these modes contribute to two vibrational bands, marked 6/1 and 1/6.

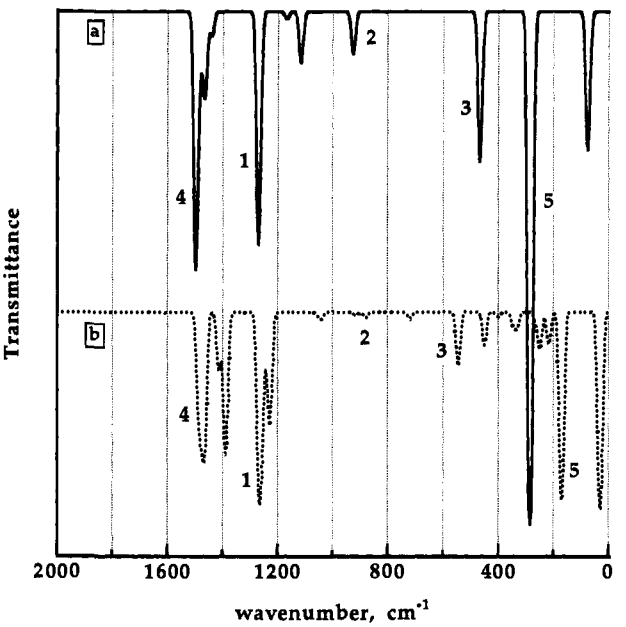

Figure 4. Calculated infrared vibrational spectra of (a) nitrosomethane hydrogen adduct and (b) 2-methyl-2-nitrosopropane hydrogen adduct. Spectra have been converted from stick spectra by the same procedure as in Figure 2. Assigned lines in the spectra are (1) NO stretch, (2) CN stretch, (3) CNO bend, (4) CNH bend, and (5) NH out-of-plane wag.

996/1161 cm^{-1} in the anion to 1271 cm^{-1} in the H adduct. The corresponding frequencies for MNP, MNP^-, and MNPH are 1600, 1110, and 1266 cm^{-1}, respectively.

The conclusion of this section is that nitrosomethane is generally a satisfactory model for 2-methyl-2-nitrosopropane, on the basis of similar molecular structures, similar reaction energies, and similar properties. On the other hand, a methyl group cannot reproduce the steric hindrance that a *tert*-butyl group provides. These differences combine with the numerical

Table 3. Electronic Energies (in hartrees) of Molecules Included in This Study as Well as Zero-Point Energies (in hartrees) and Free Energies of Solvation (in kJ mol^{-1})

molecule	E_{MP2} MP2 geom	ZPE_{SCF} (unscaled)	ΔG_{hyd}[a], kJ mol^{-1}	E_{G2}[b]	$\langle S^2\rangle$[c] (UHF)
CH_3NO nitrosomethane	−169.321 39	0.047 00	−11	−169.546 76	
CH_3NO^- nitrosomethane anion	−169.316 76	0.044 11	−297	−169.554 61	0.78
CH_3NHO methyl nitroxide	−169.900 07	0.059 63	−16	−170.134 16	0.78
CH_3NOH methylhydroxylaminyl radical	−169.889 62	0.058 91	13		0.76
CH_3NHOH methylhydroxylamine	−170.505 73	0.073 12	−16	−170.748 40	
CH_2NHO formaldonitrone	−169.322 37	0.049 03	−77	−169.547 69	
syn-CH_2NOH formaldoxime	−169.326 86	0.047 30	14		
anti-CH_2NOH formaldoxime	−169.336 81	0.047 95	7	−169.565 46	
$(CH_3)_2NO$ dimethyl nitroxide	−209.082 15	0.089 89	−10		0.78
CH_3NHO^+ N-protonated NM	−169.616 29	0.061 75	−296		
CH_3NOH^+ O-protonated NM	−169.571 95	0.059 46	−301		
CH_3NHO^- nitroxide anion	−169.902 67	0.058 44	−303		
$(CH_3)_2NO^-$ dimethyl nitroxide anion	−209.082 57	0.087 97	−295		
CH_3NHOH^+ hydroxylamine cation	−170.204 59	0.072 40	−307		0.77
trans-$(CH_3NO)_2$ nitrosomethane dimer	−338.690 52	0.100 93	18		
cis-$(CH_3NO)_2$ nitrosomethane dimer	−338.673 37	0.100 79	−106		
trans-$(CH_3NO)_2^-$ dimer anion	−338.666 27	0.095 51	−219		0.78
$CH_3NHO{-}NOCH_3$ dimer H-adduct	−339.220 13	0.114 00	12		0.78
H_2O	−76.212 30	0.022 41	−11	−76.332 05*	
OH^-	−75.590 84	0.008 58	−382	−75.712 76*	
CH_3	−39.676 73	0.031 38	14	−39.745 09*	0.76
$(CH_3)_2COH$ 2-hydroxy-2-propyl radical	−193.075 50	0.100 81	10		0.76
$(CH_3)_2COH^+$ 2-hydroxy-2-propyl cation	−192.861 11	0.103 04	−263		
$(CH_3)_2CO$ acetone	−192.554 15	0.089 97	−10		
$(CH_3)_2CO^-$ 2-oxy-2−propyl radical anion	−192.485 22	0.086 21	−286		0.77
NO	−129.573 06	0.002 82	14	−129.739 95*	0.78
HNO	−130.140 89	0.015 67	−10	−130.315 39*	
H	−0.498 23	0.000 00	19	−0.500 00*	
H^+	0.000 00	0.000 00	−1079	0.000 00	
e^-	0.000 00	0.000 00	−161	0.000 00	

[a] Free energies of hydration computed using eqs 1 and 2, except for e^-_{aq}, H^+ and H, for which data were taken from Han and Bartels.[48] [b] G2 energies marked with an asterisk were taken from Curtiss *et al.*[27] [c] $\langle S^2\rangle$ values are from UHF/6-31+G* wave functions.

uncertainties to make the present study of more qualitative than quantitative value for describing the thermodynamics of radiolyzed solutions containing MNP.

Reactions of Nitrosomethane and Its Derivatives

To provide a qualitative assessment of the probable reactions involving NM in radiolyzed aqueous solution, we have carried out extensive calculations at the MP2 level and have determined free energies of reaction at 298 K for the various processes considered. A compilation of the electronic energies and hydration free energies of the species considered here appears in Table 3. A list of the reactions of interest is given in Table 4. Since the *ab initio* calculations performed here (other than the SCRF calculations) refer to isolated molecules, these numbers are indicative of gas-phase reactions, except where adjusted by the free energies of hydration.

The energies in Table 3 are the basic data for this paper. Insight to the chemistry of spin-trap systems is obtained by combining them to obtain heats or free energies of reaction for the various possible reactions. We have applied experimental free energies of hydration for the proton, the hydrogen atom, and the hydrated electron (values taken from Han and Bartels[48]), since the SCRF approach as employed here cannot be used on these species. All other hydration free energies were calculated with self-consistent reaction fields as described above. There are, unfortunately, very few reports of experimental energies of solvation for the molecules discussed here. Species for which comparison is possible are H_2O (−8.6 kJ mol^{-1}),[49] acetone (−8.0 kJ mol^{-1}),[36] hydroxide anion (−420 kJ mol^{-1}),[37] and

(48) Han, P.; Bartels, D. M. *J. Phys. Chem.* **1990**, *94*, 7294−7299.
(49) Ben-Naim, A.; Marcus, Y. *J. Chem. Phys.* **1984**, *81*, 2016−2027.

Table 4. Calculated Free Energies of Reaction at 298 K (in kJ mol^{-1}) for Various Reactions Involving Nitrosomethane and Its Derivatives

reactions	MP2	MP2(aq)[a]	G2
Reduction Reactions			
1. $CH_3NO + H \rightarrow CH_3NHO$	−152	−176	−203
2. $CH_3NO + (CH_3)_2COH \rightarrow CH_3NHO + (CH_3)_2CO$	−151	−176	
3. $CH_3NO + CH_3 \rightarrow (CH_3)_2NO$	−150	−162	
4. $CH_3NO + e^- \rightarrow CH_3NO^-$	9	−116	−23
5. $CH_3NO + (CH_3)_2COH \rightarrow CH_3NO^- + (CH_3)_2COH^+$	572	12	
6. $CH_3NO + (CH_3)_2CO^- \rightarrow CH_3NO^- + (CH_3)_2CO$	−171	−181	
7. $CH_3NO + H \rightarrow CH_3NOH$	−124	−118	
8. $CH_3NHO + H \rightarrow CH_3NHOH$	−215	−233	−272
9. $CH_3NOH + H \rightarrow CH_3NHOH$	−243	−291	
10. $CH_3NO^- + H \rightarrow CH_3NHO^-$	−162	−188	
11. $CH_3NO^- + CH_3 \rightarrow (CH_3)_2NO^-$	−154	−166	
Disproportionation Reaction			
12. $2\ CH_3NHO \rightarrow CH_3NHOH + CH_3NO$	−62	−58	−69
Dimerization Reactions			
13. $2\ CH_3NO \rightarrow$ *trans*-$(CH_3NO)_2$	−52	−12	
14. $2\ CH_3NO \rightarrow$ *cis*-$(CH_3NO)_2$	−11	−94	
15. $CH_3NO^- + CH_3NO \rightarrow (CH_3NO)_2^-$	−9	80	
16. $CH_3NHO + CH_3NO \rightarrow CH_3NHO{-}NOCH_3$	75	114	
Reduction Reactions of Dimers			
17. $(CH_3NO)_2 + e^- \rightarrow (CH_3NO)_2^-$	52	−24	
18. $(CH_3NO)_2 + (CH_3)_2COH \rightarrow (CH_3NO)_2^- + (CH_3)_2COH^+$	615	104	
19. $(CH_3NO)_2 + H \rightarrow CH_3NHO{-}NOCH_3$	−25	−50	
Protonation Reactions			
20. $CH_3NO + H^+ \rightarrow CH_3NOH^+$	−595	194	
21. $CH_3NO + H^+ \rightarrow CH_3NHO^+$	−707	87	
22. $CH_3NO^- + H^+ \rightarrow CH_3NHO$	−1464	−104	−1495
23. $CH_3NHO^- + H^+ \rightarrow CH_3NHOH$	−1517	−150	
24. $(CH_3)_2CO + H^+ \rightarrow (CH_3)_2COH^+$	−742	84	
25. $(CH_3)_2CO^- + H^+ \rightarrow (CH_3)_2COH$	−1485	−110	
Isomerization Reactions			
26. $CH_3NO \rightarrow CH_2NHO$	5	−61	−1
27. $CH_3NO \rightarrow$ *anti*-CH_2NOH	−37	−18	−48
Other Reactions			
28. $CH_3NO \rightarrow CH_3 + NO$	118	157	130
29. $CH_3NHO \rightarrow CH_3 + HNO$	145	165	157
30. $H + OH^- \rightarrow e^- + H_2O$	−266	−85	−287
31. $H^+ + OH^- \rightarrow H_2O$	−1570	−130	−1602
32. $H^+ + e^- \rightarrow H$	−1304	−45	−1311

[a] The quantities labeled MP2(aq) contain corrections for free energies of solvation; see text and Table 3 for details.

protonated acetone (estimated to be −250 kJ mol^{-1}).[38] These values lie within the accuracies claimed earlier.

Two molecules, formaldonitrone and the *cis* dimer of nitrosomethane, have quite large free energies of hydration compared to the other neutral molecules listed. Both of these molecules have quite large gas-phase dipole moments, which interact strongly with the reaction field. The interaction is exaggerated by the mismatch between the spherical cavity and the actual shapes of these molecules. In the case of the nitrone, the zwitterionic character of the molecule is increased by interaction with the reaction field. The *cis* dimer also has a resonance structure which is capable of interacting strongly with the reaction field. In cases like these two molecules, in which one principal axis differs considerably from the others, it is no longer clear what the appropriate value of a_0 should be. This is, of course, the chief argument against the use of spherical cavities and the reason why they cannot provide quantitative predictions.

We have also reported in Table 3 the expectation value of the spin operator $\langle S^2 \rangle$ for the radicals studied. In each case the value is slightly larger than 0.75, the correct value for a true doublet state. This indicates that spin contamination by higher multiplets is slight and that the single-determinant UHF wave function is generally a satisfactory approximation for these molecules.

Numerous reactions involving NM and related molecules are presented in Table 4. For the reader's convenience, all reactions in Table 4 are numbered, and these numbers are used in the discussion. Three columns appear in Table 4, labeled MP2, MP2(aq), and G2. The MP2 column gives free energies of reaction at 298 K based upon the MP2 electronic energies of Table 3. These data are appropriate for describing gas-phase reactions. The quantities in the MP2(aq) column were derived from those in the MP2 column by adding to them the changes in free energy of hydration in going from reactants to products. The G2 column contains the most elaborate (and presumably most accurate) computations reported in this work. Not all molecules were studied at the G2 level, so only certain reactions are reported at this level. G2 free energies do not contain hydration contributions, and should be compared to the MP2 values.

Gas-phase free energy changes using MP2 tend to be within 50 kJ mol^{-1} of those using G2. This figure suggests, but does not guarantee, that the free energy changes discussed below will be within 50 kJ mol^{-1} of experimental values. There will undoubtedly be specific instances (such as the dimers discussed above) in which the MP2 description is inadequate. The reactions themselves can be classified under a number of general headings.

Reduction of Nitrosomethane. This category includes direct reduction by electron transfer and the spin-trapping reaction itself. Spin trapping of a hydrogen atom (reaction 1) is an

energetically favorable process, as is that of methyl radical (reaction 3) ($\Delta G^\circ = -152$ and -150 kJ mol^{-1}, respectively, using gas-phase MP2 free energies). Hydrogen trapping is slightly more favored in solution due to the larger positive free energy of solvation of H. Direct reduction of NM by electron capture (reaction 4) is slightly thermodynamically disfavored, and by electron transfer from 2-hydroxy-2-propyl radical (reaction 5) it is substantially disfavored in the gas phase ($\Delta G^\circ = 9$ and $+572$ kJ mol^{-1}, respectively). (2-Hydroxy-2-propyl radical is abundantly produced when 2-propanol is present in radiolyzed aqueous solution, and it is frequently used as a reducing agent). In solution, the analogue of the free electron is the hydrated electron, whose high reactivity drives the reaction in the direction of reduction. Reduction by the hydroxypropyl radical becomes much less unfavorable ($\Delta G^\circ_5 = +12$ kJ mol^{-1}), due to the production and solvation of a pair of ions. Reduction by the conjugate base of the hydroxypropyl radical is quite exoergic both in the gas phase and in solution ($\Delta G^\circ_6 = -171$ and -181 kJ mol^{-1}, respectively), but the base is only likely to be present at rather high pH. Reduction by transfer of a hydrogen atom seems to be a favorable method of depleting nitrosomethane. For instance, $\Delta G^\circ_2 = -151$ kJ mol^{-1} when 2-hydroxy-2-propyl radical is used as the hydrogen donor.

It is useful to compare the reactions which produce the reduced species MNH with those which produce NM$^-$, inasmuch as the reducing agents in the latter instance can be considered the conjugate bases of the hydrogen-atom transfer reagents. For example, the equilibria

$$H^+(aq) + e^-(aq) \rightleftarrows H(aq)$$

and

$$H^+(aq) + (CH_3)_2CO^-(aq) \rightleftarrows (CH_3)_2COH(aq)$$

suggest that reduction of NM to NM$^-$ will prevail in basic solution, whereas reduction by hydrogen attack will be favored in acidic media. The initial reduction reactions 1 and 6 are comparably exoergic, indicating that considerable NM$^-$ may be present in basic or neutral radiolyzed aqueous solution. Protonation of NM$^-$ to give NMH is favored. Interestingly, the methyl radical affinity of NM$^-$ is comparable to that of NM ($\Delta G^\circ_{11} = -154$ *vs* $\Delta G^\circ_3 = -150$ kJ mol^{-1}), indicating the likelihood of spin trapping regardless of pH. Indeed, in the competition between production of dialkyl nitroxide and monoalkyl nitroxide, the latter will be suppressed as the pH rises.

It is also possible for a hydrogen atom to associate with the oxygen of the nitroso group rather than with the nitrogen (reaction 7). Production of this radical is 28 kJ mol^{-1} less exoergic than the expected nitroxide (reaction 1), and CH_3NOH has not to our knowledge been observed.

The continuing reduction of the nitroxide to hydroxylamine is apparently even more exoergic ($\Delta G^\circ_8 = -215$ kJ mol^{-1}) than the initial spin-trapping reaction 1. The disproportionation reaction

$$2CH_3NHO \rightarrow CH_3NHOH + CH_3NO$$

has $\Delta G^\circ_{12} = -62$ kJ mol^{-1} and could contribute to the reduction process at sufficiently large concentrations of nitroxide.

Dimerization of Nitrosomethane and Related Species. Dimerization of NM (reactions 13 and 14) is an instance in which the SCF description is completely inadequate, and the MP2 description is also less than satisfactory. Heiberg[12,50] has pointed out the role of certain electronic configurations in accurately describing the wave functions of both the dimer and its dissociative transition state; among these is a configuration which corresponds to a 4-electron excitation relative to the dimer's ground state. Such a contribution is not accommodated by the MP2 approximation, resulting in an unsatisfactory description of $(NM)_2$ at the MP2 level. Note, however, that this difficulty does not carry over to the pseudodimer molecules $(NM)_2^-$ and NM−NMH, since in each of them the ONNO π system has been disrupted, namely, one of the nitrogens has been converted to sp^3 bonding. The consequence for the present work is that all calculations on reactions involving $(NM)_2$ underestimate the stability of $(NM)_2$ relative to the other components of the reaction. Heiberg's configuration interaction energies[12] combined with the present thermodynamic correction terms imply a free energy of dimerization for the *trans* dimer about 10 kJ mol^{-1} more negative than indicated in Table 4.

MP2 results give $\Delta G^\circ_{13} = -52$ kJ mol^{-1} for production of the *trans* dimer and $\Delta G^\circ_{14} = -11$ kJ mol^{-1} for the *cis* dimer of nitrosomethane. These are both underestimates of the actual exoergicity of these processes, as pointed out above. Note that the free energies in solution indicate the *cis* dimer to be strongly favored over the *trans*. This is in part an artifact of the SCRF solvation model in use: Since the *trans* dimer has no dipole moment, it does not interact with the reaction field and thus has a small positive free energy of solvation arising from the last three terms in eq 2. The chemically similar *cis* dimer has a rather large dipole moment, and a considerable free energy of hydration. A more sophisticated SCRF model would account for the polarities of the constituent groups in *trans*-$(NM)_2$ to produce a less positive and possibly negative free energy of solvation.

We have also explored the pseudodimerization reactions of NM + NM$^-$ (reaction 15) and NM + NMH (methyl nitroxide) (reaction 16) to give the reduced forms of the $(NM)_2$ dimer. The anionic process is slightly exoergic ($\Delta G^\circ_{15} = -9$ kJ mol^{-1}) in the gas phase, but quite destabilized in solution, due to the greater solvation energy of the smaller NM$^-$ ion. The neutral process is disfavored by 75 kJ mol^{-1} in the gas phase and even more in solution.

Reduction of Nitrosomethane Dimers. Reduction of $(NM)_2$ to $(NM)_2^-$ by electron transfer is disfavored in the gas phase for any of the reducing agents examined here. In solution reduction by the hydrated electron is exoergic ($\Delta G^\circ_{17} = -24$ kJ mol^{-1}), and a reaction of some sort between the analogous $(MNP)_2$ molecule and the hydrated electron has been reported to occur.[3] In electrochemical measurements,[5] reduction of $(MNP)_2$ in aqueous or acetonitrile solution is not observed prior to the onset of solvent discharge. Reduction of $(NM)_2$ by H atom to produce the NMH−NM "dimer" is exoergic by 25 kJ mol^{-1} in the gas phase and by 50 kJ mol^{-1} in solution, indicating that $(NM)_2$ can function as a spin trap in solution. Although the free energy of the reaction $(NM)_2 + H \rightarrow$ NM−NMH is much less negative than that of NM + H → NMH (-50 *vs* -176 kJ mol^{-1} in solution), under some circumstances the concentration of $(NM)_2$ may be higher than that of NM, allowing the dimer to play a role in primary radical depletion. However, as we have seen above, once the dimer traps a radical molecule, it is likely to dissociate to the monomer and the nitroxide. Thus the same products are going to be formed whether a monomer or a dimer does the actual trapping. This will simplify radical identification but complicate the kinetic analysis of time-resolved ESR data. Dissociation is also likely to be the fate of any dimer

(50) Heiberg, A. B. *Chem. Phys.* **1977**, *26*, 309.

anion formed, e.g.,

$$(CH_3NO)_2 + e_{aq}^- \rightarrow CH_3NO + CH_3NO^- \qquad \Delta G^\circ = -104 \text{ kJ mol}^{-1}$$

This may be the reaction that Kuwabara *et al.* observe.[3] The driving force is much less when electron donors other than the hydrated electron are considered e.g., $\Delta G^\circ_{18} = 104$ kJ mol^{-1} in solution.

Protonation Reactions. In these cases the gas-phase and solution results differ dramatically, because of the huge (−1079 kJ mol^{-1}) solvation free energy of H^+. In solution, the protonation of NM (reactions 20 and 21) appears to be endoergic, and much less likely to occur at the oxygen than the nitrogen atom. Capture of a proton by NM^- is exoergic ($\Delta G^\circ_{22} = -104$ kJ mol^{-1}), however. Neutralization of the conjugate base of hydroxylamine is favored ($\Delta G^\circ_{23} = -150$ kJ mol^{-1}). The pK_as for proton loss from CH_3NHO^+, CH_3NHO, and CH_3NHOH are calculated to be −15.2, 18.1, and 26.1, respectively. However, the estimated errors of ±24 kJ mol^{-1} in solvation free energies of ionic molecules noted earlier imply errors in pK_a of ±5, so only the ordering of the pK_as presented here is likely to have significance.

Also included in this section are the acid dissociations of 2-hydroxy-2-propyl radical (reaction 25) and the corresponding cation (reaction 24). The calculated data imply pK_a values of +19.2 and −14.6, respectively, whereas experimental reports are +12.0[51] and −7.2.[52] Lim *et al.*[53] have pointed out the consequences of inaccurate solvation energies in estimating pK_as, and the present results emphasize this problem.

Isomerization Reactions. The isomerization of NM to the nitrone structure (reaction 26) has a free energy change of essentially zero. The *anti* rotamer of the oxime structure is 37 kJ mol^{-1} lower in free energy than NM (reaction 27). Very little is known about the energetics of these processes, although NM converts to the oxime in minutes at a temperature of about 160 °C in the gas phase.[54] Adeney *et al.*[10] examined nitrosomethane, formaldonitrone, and formaldoxime at the MP3/6-31G++ level and reported that the electronic energy of the nitrone was 51.6 kJ mol^{-1} above that of NM and that of the oxime 40.8 kJ mol^{-1} below. It is not clear why Adeney's and the present calculations differ so widely (by 47 kJ mol^{-1}) only for the relative energy of the nitrone. The G2 results of Table 4 support the present MP2 results over those of Adeney *et al.* There are no comparable isomerization reactions in MNP. In solution the relative stabilities of nitrone and oxime are reversed, due to a very large free energy of solvation of nitrone.

Other Reactions. The dissociation of NM is of interest in that MNP is known to photodissociate and to dissociate in the dark in aqueous solution, thereby providing *tert*-butyl radicals which interact with MNP to produce di-*tert*-butyl nitroxide. The gas-phase dissociation of NM is disfavored according to the present results ($\Delta G^\circ_{28} = +118$ kJ mol^{-1}); that of MNP would be less so because of the greater stabilization of the *tert*-butyl radical relative to methyl. The experimental free energy of dissociation of NM is 114 kJ mol^{-1} in the gas phase,[55] in excellent agreement with the MP2 gas-phase result.

The hydrogen atom−hydrated electron equilibrium is important in radiolyzed aqueous solutions, and recent experimental determinations[48] afford a test of the electronic and solvation energies of OH^- and H_2O used here. The theoretical value of $\Delta G^\circ_{30} = -85$ kJ mol^{-1} can be compared to the experimental determination of −25 kJ mol^{-1}, indicative of the sort of agreement we expect at this level of theory. The other two fundamental reactions listed, the ionic dissociation of water (reaction 31) and the conversion of hydrated electron to hydrogen atom (reaction 32), are dominated by our choice of hydration free energies. The experimental values in aqueous solution are −80 kJ mol^{-1} for the former (from $K_{diss} = [H^+_{aq}][OH^-_{aq}] = 10^{-14}$) and −55 kJ mol^{-1} for the latter,[48] compared to our theoretical values of −130 and −45 kJ mol^{-1}.

Conclusions

The radiolysis of aqueous solutions containing nitroso spin-trap molecules produces a considerable array of transients and products, the identities of which are by no means well-established. In this work we have sought to learn, on energetic grounds, whether some of the postulated transient molecules are potential promoters or competitors of the spin-trapping reactions. The nitrosoalkane dimer, for instance, is capable of acting as a spin trap in its own right, but once it traps a radical, it is prone to dissociate to the monomer and the nitroxide radical. The dimer anion also appears unstable with respect to dissociation into a neutral monomer and a monomer anion. The monomer anion can be readily produced by reaction with hydrated electrons or other strong reducing agents and can be depleted by capture of protons or hydrogen atoms to produce respectively the nitroxide or the hydroxylamine conjugate base. It also appears capable of trapping organic radicals to produce the dialkylhydroxylamine conjugate base. In terms of the spin-trapping process, most paths lead to the nitroxide radical, but the mechanisms by which they arrive there are quite varied and likely to produce complicated kinetics. The answer to the question posed in the Introduction is that both the dimer and reduced monomer appear capable of participating in spin-trapping reactions, but experimental characterization of their participation may prove challenging.

Having said this, we must point out that all our conclusions are based on the thermodynamics of the molecules studied. Kinetic factors, such as the heights of barriers to reaction or the steric shielding effects of *tert*-butyl groups, will certainly play a role in determining which reactions actually take place. Our work is a first step in the theoretical study of spin trapping by nitroso compounds. Further refinement to provide quantitative rather than qualitative results will require a larger basis set than employed here, correlation effects beyond the MP2 level, and a much more sophisticated treatment of free energies of solvation. Some of the questions of reaction kinetics are addressable, in principle, through the computation of transition-state structures and energies, although determination of solvation energies for transition states will be an extremely difficult problem.

A subsidiary conclusion of this work is that, in experimental studies of solutions containing nitroso spin traps, the NO stretch vibrational frequency will be diagnostic of the state of reduction, protonation, or dimerization of the spin-trap molecule. Although the vibrational frequencies reported here are not in quantitative agreement with experiment, they show variations of several hundred reciprocal centimeters for the NO stretch in different chemical environments. This large range may expedite experimental characterization of some of the radical species considered here.

(51) Laroff, G. P.; Fessenden, R. W. *J. Phys. Chem.* **1973**, *77*, 1283–1288.
(52) Stewart, R. *The Proton: Application to Organic Chemistry*; Academic Press: New York, 1985.
(53) Lim, C.; Bashford, D.; Karplus, M. *J. Phys. Chem.* **1991**, *95*, 5610–5620.
(54) Lüttke, W. *Z. Elektrochem., Ber. Bunsenges. Phys. Chem.* **1957**, *61*, 302–313.
(55) Jodkowski, J. T.; Ratajczak, E.; Sillesen, A.; Pagsberg, P. *Chem. Phys. Lett.* **1993**, *203*, 490–496.

Acknowledgment. We are grateful to Dr. D. M. Chipman and Professors R. W. Fessenden and B. G. Gowenlock for their helpful comments. The research described herein was supported by the Office of Basic Energy Sciences of the U.S. Department of Energy. This is contribution No. NDRL-3664 from the Notre Dame Radiation Laboratory. Some of the calculations reported here were performed on a Convex C240 in Notre Dame's Office of University Computing, whose support we appreciate.